ISSN 2581 – 3781

AJCSE
ASIAN JOURNAL OF COMPUTER SCIENCE ENGINEERING

Available Online at www.ajcse.info
Asian Journal of Computer Science Engineering 2021;6(4):46-54

REVIEW ARTICLE

On increasing of the Density of Elements of Field-effect Heterotransistors Framework a Four-stage Distributed Amplifier: Accounting of Mismatch-induced Stress and Porosity of Materials

E. L. Pankratov[1,2]

[1]*Department of Mathematical and Natural Sciences, Nizhny Novgorod State University, Nizhny Novgorod, Russia,*
[2]*Department of Higher Mathematics, Nizhny Novgorod State Technical University, Nizhny Novgorod, Russia*

Received on: 29-10-2021; Revised on: 30-11-2021; Accepted on: 13-12-2021

ABSTRACT

In this paper, we introduce an approach to increase the density of field-effect transistors framework a four-stage distributed amplifier. Framework the approach, we consider manufacturing the amplifier in heterostructure with specific configuration. Several required areas of the heterostructure should be doped by diffusion or ion implantation. After that, dopant and radiation defects should by annealed framework optimized scheme. We also consider an approach to decrease value of mismatch-induced stress in the considered heterostructure. We introduce an analytical approach to analyze mass and heat transport in heterostructures during manufacturing of integrated circuits with account mismatch-induced stress.

Key words: Analytical approach for modeling, Four-stage distributed amplifier, Optimization of manufacturing, Accounting of mismatch-induced stress and porosity of materials

INTRODUCTION

In the present time, several actual problems of the solid-state electronics (such as increasing of performance, reliability, and density of elements of integrated circuits: Diodes, field-effect, and bipolar transistors) are intensively solving.[1-6] To increase the performance of these devices, it is attracted an interest determination of materials with higher values of charge carriers mobility.[7-10] One way to decrease dimensions of elements of integrated circuits is manufacturing them in thin film heterostructures.[3-5,11] In this case, it is possible to use inhomogeneity of heterostructure and necessary optimization of doping of electronic materials[12] and development of epitaxial technology to improve these materials (including analysis of mismatch-induced stress).[13-15] An alternative approach to increase dimensions of integrated circuits is using of laser and microwave types of annealing.[16-18]
Framework the paper, we introduce an approach to manufacture field-effect transistors. The approach gives a possibility to decrease their dimensions with increasing their density framework a four-stage distributed amplifier. We also consider possibility to decrease mismatch-induced stress to decrease quantity of defects, generated due to the stress. In this paper, we consider a heterostructure, which consist of a substrate and an epitaxial layer [Figure 1]. We also consider a buffer layer between the substrate and the epitaxial layer. The epitaxial layer includes into itself several sections, which were manufactured using another material. These sections have been doped by diffusion or ion implantation to manufacture the required types of conductivity (*p* or *n*). These areas became sources, drains, and gates [Figure 1]. After this doping, it is required annealing of dopant and/or radiation defects. The main aim of the present paper is analysis of redistribution of dopant and radiation defects to determine conditions, which correspond to decreasing of elements of the considered amplifier and at the same time to increase their density. At the same time, we consider a possibility to decrease mismatch-induced stress.

Address for correspondence:
E. L. Pankratov
E-mail: elp2004@mail.ru

METHOD OF SOLUTION

To solve our aim, we determine and analyzed spatiotemporal distribution of the concentration

of dopant in the considered heterostructure. We determine the distribution by solving the second Fick's law in the following form.[1,20-23]

$$\frac{\partial C(x,y,z,t)}{\partial t}=\frac{\partial}{\partial x}\left[D\frac{\partial C(x,y,z,t)}{\partial x}\right]+$$
$$\frac{\partial}{\partial y}\left[D\frac{\partial C(x,y,z,t)}{\partial y}\right]+\frac{\partial}{\partial z}\left[D\frac{\partial C(x,y,z,t)}{\partial z}\right]+$$
$$+\Omega\frac{\partial}{\partial x}\left[\frac{D_S}{kT}\nabla_S\mu_1(x,y,z,t)\int_0^{L_z}C(x,y,W,t)\,dW\right]+$$
$$+\Omega\frac{\partial}{\partial y}\left[\frac{D_S}{kT}\nabla_S\mu_1(x,y,z,t)\int_0^{L_z}C(x,y,W,t)\,dW\right]+ \quad (1)$$
$$+\frac{\partial}{\partial x}\left[\frac{D_{CS}}{\bar{V}kT}\frac{\partial\mu_2(x,y,z,t)}{\partial x}\right]+$$
$$\frac{\partial}{\partial y}\left[\frac{D_{CS}}{\bar{V}kT}\frac{\partial\mu_2(x,y,z,t)}{\partial y}\right]+$$
$$\frac{\partial}{\partial z}\left[\frac{D_{CS}}{\bar{V}kT}\frac{\partial\mu_2(x,y,z,t)}{\partial z}\right]$$

with boundary and initial conditions

$$\left.\frac{\partial C(x,y,z,t)}{\partial x}\right|_{x=0}=0,\ \left.\frac{\partial C(x,y,z,t)}{\partial x}\right|_{x=L_x}=0,$$

$$\left.\frac{\partial C(x,y,z,t)}{\partial y}\right|_{y=0}=0,\ C(x,y,z,0)=f_C(x,y,z),$$

$$\left.\frac{\partial C(x,y,z,t)}{\partial y}\right|_{x=L_y}=0,\ \left.\frac{\partial C(x,y,z,t)}{\partial z}\right|_{z=0}=0,$$

$$\left.\frac{\partial C(x,y,z,t)}{\partial z}\right|_{x=L_z}=0.$$

Here, $C(x,y,z,t)$ is the spatiotemporal distribution of the concentration of dopant; Ω is the atomic volume of dopant; ∇_s is the symbol of surficial gradient; $\int_0^{L_z}C(x,y,z,t)\,dz$ is the surficial concentration of dopant on interface between layers of heterostructure (in this situation, we assume that Z-axis is perpendicular to interface between layers of heterostructure); $\mu_1(x,y,z,t)$ and $\mu_2(x,y,z,t)$ are the chemical potential due to the presence of mismatch-induced stress and porosity of material; and D and D_S are the coefficients of volumetric and surficial diffusions. Values of dopant diffusions coefficients depend on properties of materials of heterostructure, speed of heating and cooling of materials during annealing, and spatiotemporal distribution of concentration of dopant. Dependences of dopant diffusions coefficients on parameters could be approximated by the following relations.[24-26]

$$D_C=D_L(x,y,z,T)\left[1+\xi\frac{C^\gamma(x,y,z,t)}{P^\gamma(x,y,z,T)}\right]$$
$$\left[1+\varsigma_1\frac{V(x,y,z,t)}{V^*}+\varsigma_2\frac{V^2(x,y,z,t)}{(V^*)^2}\right],$$

$$D_S=D_{SL}(x,y,z,T)\left[1+\xi_S\frac{C^\gamma(x,y,z,t)}{P^\gamma(x,y,z,T)}\right]$$
$$\left[1+\varsigma_1\frac{V(x,y,z,t)}{V^*}+\varsigma_2\frac{V^2(x,y,z,t)}{(V^*)^2}\right]. \quad (2)$$

Here, $D_L(x,y,z,T)$ and $D_{LS}(x,y,z,T)$ are the spatial (due to accounting all layers of heterostructure) and temperature (due to Arrhenius law) dependences of dopant diffusion coefficients; T is the temperature of annealing; $P(x,y,z,T)$ is the limit of solubility of dopant; parameter γ depends on properties of materials and could be integer in the following interval $\gamma\in[1,3]$;[24] $V(x,y,z,t)$ is the spatiotemporal distribution of concentration of radiation vacancies; and V^* is the equilibrium distribution of vacancies. Concentrational dependence of dopant diffusion coefficient has been described in details in Gotra.[24] Spatiotemporal distributions of the concentration of point radiation defects have been determined by solving the following system of equations.[20-23,25,26]

$$\frac{\partial\rho(x,y,z,t)}{\partial t}=\frac{\partial}{\partial x}\left[D_\rho(x,y,z,T)\frac{\partial\rho(x,y,z,t)}{\partial x}\right]$$
$$+\frac{\partial}{\partial y}\left[D_\rho(x,y,z,T)\frac{\partial\rho(x,y,z,t)}{\partial y}\right]+$$
$$+\frac{\partial}{\partial z}\left[D_\rho(x,y,z,T)\frac{\partial\rho(x,y,z,t)}{\partial z}\right]-k_{\rho,\rho}$$
$$(x,y,z,T)\,\rho^2(x,y,z,t)-k_{I,V}(x,y,z,T)\times$$

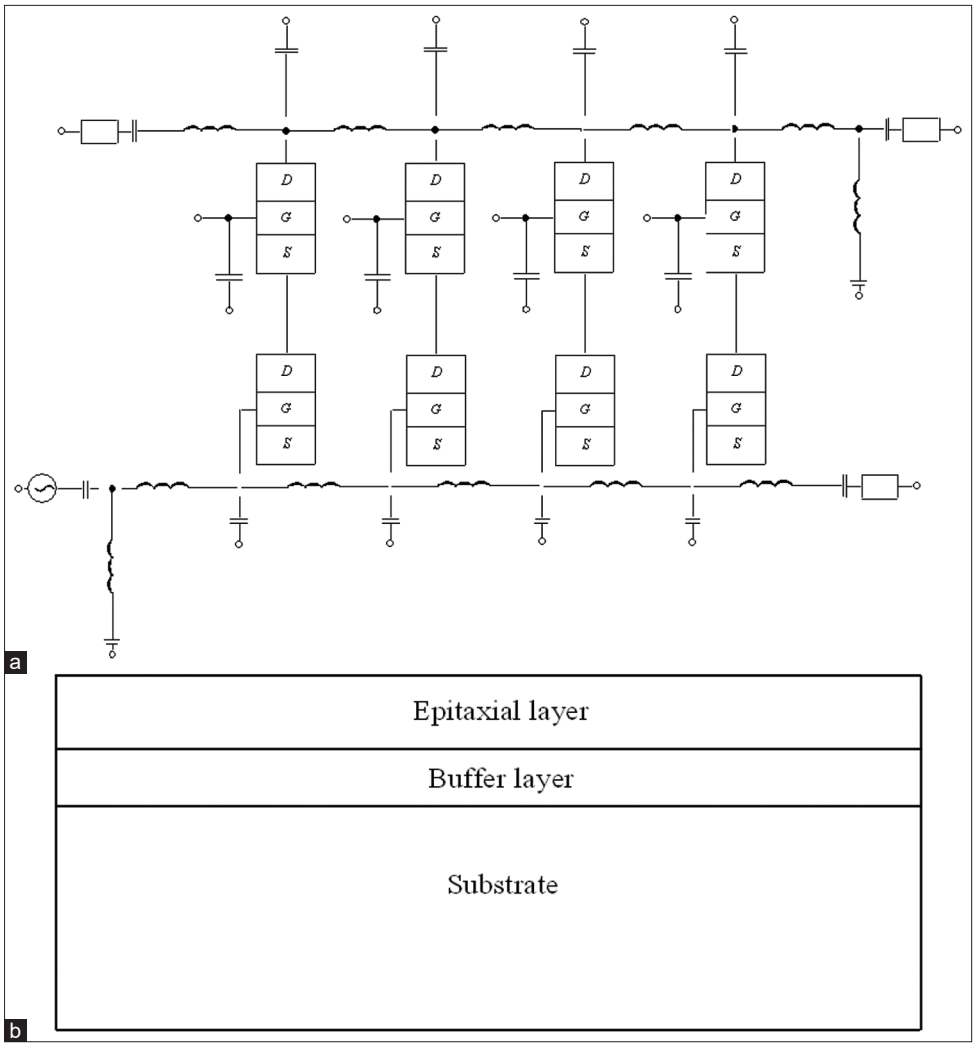

Figure 1: (a) Structure of the considered amplifier.[19] (b) Heterostructure with a substrate, epitaxial layers, and buffer layer (view from side)

$$\times I(x,y,z,t)V(x,y,z,t)+\Omega\frac{\partial}{\partial x}$$

$$\left[\frac{D_{\rho S}}{kT}\nabla_S\mu\,(x,y,z,t)\int_0^{L_z}\rho(x,y,W,t)\,dW\right]+$$

$$+\Omega\frac{\partial}{\partial y}\left[\frac{D_{\rho S}}{kT}\nabla_S\mu\,(x,y,z,t)\int_0^{L_z}\rho(x,y,W,t)\,dW\right]$$

$$+\frac{\partial}{\partial x}\left[\frac{D_{\rho S}}{\bar{V}\,kT}\frac{\partial\mu_2(x,y,z,t)}{\partial x}\right]+$$

$$+\frac{\partial}{\partial y}\left[\frac{D_{\rho S}}{\bar{V}\,kT}\frac{\partial\mu_2(x,y,z,t)}{\partial y}\right]$$

$$+\frac{\partial}{\partial z}\left[\frac{D_{\rho S}}{\bar{V}\,kT}\frac{\partial\mu_2(x,y,z,t)}{\partial z}\right] \qquad (3)$$

with boundary and initial conditions

$$\left.\frac{\partial\rho(x,y,z,t)}{\partial x}\right|_{x=0}=0,\ \left.\frac{\partial\rho(x,y,z,t)}{\partial x}\right|_{x=L_x}=0,$$

$$\left.\frac{\partial\,\rho(x,y,z,t)}{\partial y}\right|_{y=0}=0\ ,$$

$$\left.\frac{\partial\rho(x,y,z,t)}{\partial y}\right|_{y=L_y}=0,\ \left.\frac{\partial\rho(x,y,z,t)}{\partial z}\right|_{z=0}=0,$$

$$\left.\frac{\partial\rho(x,y,z,t)}{\partial z}\right|_{z=L_z}=0, \qquad (4)$$

$$\rho\,(x,y,z,0)=f_V\,(x,y,z),$$

$$V\left(x_1+V_nt,y_1+V_nt,z_1+V_nt,t\right)$$

$$=V_\infty\left(1+2\,\omega/kT\sqrt{x_1^2+y_1^2+z_1^2}\right).$$

Here, $\rho=I,V$; I (x,y,z,t) is the spatiotemporal distribution of concentration of radiation interstitials; I^* is the equilibrium distribution of interstitials; $D_I(x,y,z,T)$, $D_V(x,y,z,T)$, $D_{IS}(x,y,z,T)$, and $D_{VS}(x,y,z,T)$ are the coefficients of volumetric and surficial diffusions of interstitials and vacancies, respectively; terms $V^2(x,y,z,t)$ and $I^2(x,y,z,t)$ correspond to the generation of divacancies and diinterstitials, respectively (for example Vinetskiy and Kholodar,[26] and appropriate references in this book); $k_{I,V}(x,y,z,T)$, $k_{I,I}(x,y,z,T)$, and $k_{V,V}(x,y,z,T)$ are the parameters of recombination of point radiation defects and generation of their complexes; k is the Boltzmann constant; $\omega = a^3$, a is the interatomic distance; and l is the specific surface energy. To account porosity of buffer layers, we assume that porous is approximately cylindrical with average values $r = \sqrt{x_1^2 + y_1^2}$ and z_1 before annealing.[23] With time, small pores decomposing on vacancies. The vacancies absorbing by larger pores.[27] With time, large pores became larger due to absorbing the vacancies and became more spherical.[27] Distribution of the concentration of vacancies in heterostructure, existing due to porosity, could be determined by summing on all pores, that is,

$$V(x,y,z,t) = \sum_{i=0}^{l}\sum_{j=0}^{m}\sum_{k=0}^{n} V_p\left(\begin{matrix} x+i\alpha, y+ \\ j\beta, z+k\chi, t \end{matrix}\right),$$

$$R = \sqrt{x^2+y^2+z^2}\ .$$

Here, α, β, and χ are the average distances between centers of pores in directions x, y, and z; l, m, and n are the quantity of pores inappropriate directions. Spatiotemporal distributions of divacancies Φ_V (x,y,z,t) and diinterstitials Φ_I (x,y,z,t) could be determined by solving the following system of equations.[25,26]

$$\frac{\partial \Phi_\rho(x,y,z,t)}{\partial t} = \frac{\partial}{\partial x}\left[D_{\Phi_\rho}(x,y,z,T)\frac{\partial \Phi_\rho(x,y,z,t)}{\partial x}\right]$$
$$+\frac{\partial}{\partial y}\left[D_{\Phi_\rho}(x,y,z,T)\frac{\partial \Phi_\rho(x,y,z,t)}{\partial y}\right]+$$
$$+\frac{\partial}{\partial z}\left[D_{\Phi_\rho}(x,y,z,T)\frac{\partial \Phi_\rho(x,y,z,t)}{\partial z}\right]+\Omega\frac{\partial}{\partial x}$$
$$\left[\frac{D_{\Phi_\rho S}}{kT}\nabla_S\mu_1(x,y,z,t)\int_0^{L_z}\Phi_\rho(x,y,W,t)\,dW\right]+$$
$$+\Omega\frac{\partial}{\partial y}\left[\frac{D_{\Phi_\rho S}}{kT}\nabla_S\mu_1(x,y,z,t)\int_0^{L_z}\Phi_\rho(x,y,W,t)\,dW\right]$$
$$+k_{\rho,\rho}(x,y,z,T)\rho^2(x,y,z,t)+$$
$$+\frac{\partial}{\partial x}\left[\frac{D_{\Phi_\rho S}}{\bar{V}\,kT}\frac{\partial \mu_2(x,y,z,t)}{\partial x}\right]+$$
$$\frac{\partial}{\partial y}\left[\frac{D_{\Phi_\rho S}}{\bar{V}\,kT}\frac{\partial \mu_2(x,y,z,t)}{\partial y}\right]+$$
$$\frac{\partial}{\partial z}\left[\frac{D_{\Phi_\rho S}}{\bar{V}\,kT}\frac{\partial \mu_2(x,y,z,t)}{\partial z}\right]+$$
$$+k_\rho(x,y,z,T)\rho(x,y,z,t) \qquad (5)$$

with boundary and initial conditions

$$\left.\frac{\partial \Phi_\rho(x,y,z,t)}{\partial x}\right|_{x=0} = 0\ , \qquad \left.\frac{\partial \Phi_\rho(x,y,z,t)}{\partial x}\right|_{x=L_x} = 0\ ,$$
$$\left.\frac{\partial \Phi_\rho(x,y,z,t)}{\partial y}\right|_{y=0} = 0\ ,$$
$$\left.\frac{\partial \Phi_\rho(x,y,z,t)}{\partial y}\right|_{y=L_y} = 0\ , \qquad \left.\frac{\partial \Phi_\rho(x,y,z,t)}{\partial z}\right|_{z=0} = 0\ ,$$
$$\left.\frac{\partial \Phi_\rho(x,y,z,t)}{\partial z}\right|_{z=L_z} = 0\ , \qquad (6)$$

$\Phi^\rho(x,y,z,0)=f_{\Phi\rho}(x,y,z)$.

Here, $D_{\Phi I}(x,y,z,T)$, $D_{\Phi V}(x,y,z,T)$, $D_{\Phi IS}(x,y,z,T)$, and $D_{\Phi VS}(x,y,z,T)$ are the coefficients of volumetric and surficial diffusions of complexes of radiation defects; $k_I(x,y,z,T)$ and $k_V(x,y,z,T)$ are the parameters of decay of complexes of radiation defects.

Chemical potential μ_1 in Equation (1) could be determined by the following relation.[20]

$$\mu_1 = E(z)\Omega\sigma_{ij}[u_{ij}(x,y,z,t)+u_{ji}(x,y,z,t)]/2, \qquad (7)$$

Where, $E(z)$ is the Young modulus, σ_{ij} is the stress tensor; $u_{ij} = \frac{1}{2}\left(\frac{\partial u_i}{\partial x_j}+\frac{\partial u_j}{\partial x_i}\right)$ is the deformation tensor; u_i and u_j are the components $u_x(x,y,z,t)$, $u_y(x,y,z,t)$, and $u_z(x,y,z,t)$ of the displacement vector $\vec{u}(x,y,z,t)$; and x_i and x_j are the coordinate

x, y, and z. The Equation (3) could be transformed to the following form.

$$\mu\left(x,y,z,t\right)=\left[\frac{\partial u_i\left(x,y,z,t\right)}{\partial x_j}+\frac{\partial u_j\left(x,y,z,t\right)}{\partial x_i}\right]$$

$$\left\{\frac{1}{2}\left[\frac{\partial u_i\left(x,y,z,t\right)}{\partial x_j}+\frac{\partial u_j\left(x,y,z,t\right)}{\partial x_i}\right]-\right.$$

$$\left.\begin{matrix}-\varepsilon_0\delta_{ij}+\dfrac{\sigma\left(z\right)\delta_{ij}}{1-2\sigma\left(z\right)}\left[\dfrac{\partial u_k\left(x,y,z,t\right)}{\partial x_k}-3\varepsilon_0\right]\\ -K\left(z\right)\beta\left(z\right)\left[T\left(x,y,z,t\right)-T_0\right]\delta_{ij}\end{matrix}\right\}\frac{\Omega}{2}E\left(z\right),$$

Where, σ is Poisson coefficient; $\varepsilon_0 = (a_s\text{-}a_{EL})/a_{EL}$ is the mismatch parameter; a_s and a_{EL} are lattice distances of the substrate and the epitaxial layer; K is the modulus of uniform compression; β is the coefficient of thermal expansion; and T_r is the equilibrium temperature, which coincide (for our case) with room temperature. Components of displacement vector could be obtained by solution of the following equations.[21]

$$\begin{cases}\rho\left(z\right)\dfrac{\partial^2 u_x\left(x,y,z,t\right)}{\partial t^2}=\dfrac{\partial\sigma_{xx}\left(x,y,z,t\right)}{\partial x}+\\ \dfrac{\partial\sigma_{xy}\left(x,y,z,t\right)}{\partial y}+\dfrac{\partial\sigma_{xz}\left(x,y,z,t\right)}{\partial z}\\ \rho\left(z\right)\dfrac{\partial^2 u_y\left(x,y,z,t\right)}{\partial t^2}=\dfrac{\partial\sigma_{yx}\left(x,y,z,t\right)}{\partial x}+\\ \dfrac{\partial\sigma_{yy}\left(x,y,z,t\right)}{\partial y}+\dfrac{\partial\sigma_{yz}\left(x,y,z,t\right)}{\partial z}\\ \rho\left(z\right)\dfrac{\partial^2 u_z\left(x,y,z,t\right)}{\partial t^2}=\dfrac{\partial\sigma_{zx}\left(x,y,z,t\right)}{\partial x}+\\ \dfrac{\partial\sigma_{zy}\left(x,y,z,t\right)}{\partial y}+\dfrac{\partial\sigma_{zz}\left(x,y,z,t\right)}{\partial z}\end{cases} \quad (8)$$

Where,

$$\sigma_{ij}=\frac{E\left(z\right)}{2\left[1+\sigma\left(z\right)\right]}\left[\begin{matrix}\dfrac{\partial u_i\left(x,y,z,t\right)}{\partial x_j}\\ +\dfrac{\partial u_j\left(x,y,z,t\right)}{\partial x_i}\\ -\dfrac{\delta_{ij}}{3}\dfrac{\partial u_k\left(x,y,z,t\right)}{\partial x_k}\end{matrix}\right]+K\left(z\right)\delta_{ij}\times$$

$$\times\frac{\partial u_k\left(x,y,z,t\right)}{\partial x_k}-\beta\left(z\right)K\left(z\right)\left[T\left(x,y,z,t\right)-T_r\right],$$

$\rho\ (z)$ is the density of materials of heterostructure, and δ_{ij} is the Kronecker symbol. Conditions for the system of Equations (8) could be written in the form

$$\frac{\partial\,\vec{u}\left(0,y,z,t\right)}{\partial x}=0;\ \frac{\partial\vec{u}\left(L_x,y,z,t\right)}{\partial x}=0;$$

$$\frac{\partial\,\vec{u}\left(x,0,z,t\right)}{\partial y}=0;\ \frac{\partial\,\vec{u}\left(x,L_y,z,t\right)}{\partial y}=0;$$

$$\frac{\partial\,\vec{u}\left(x,y,0,t\right)}{\partial z}=0;\frac{\partial\,\vec{u}\left(x,y,L_z,t\right)}{\partial z}=0;$$

$$\vec{u}\left(x,y,z,0\right)=\vec{u}_0;\ \vec{u}\left(x,y,z,\infty\right)=\vec{u}_0.$$

We calculate spatiotemporal distributions of concentrations of dopant and radiation defects by solving the Equations (1), (3), (5), and (8) framework standard method of averaging of function corrections.[28] Framework this paper, we determine the concentration of dopant, concentrations of radiation defects, and components of displacement vector using the second-order approximation framework method of averaging of function corrections. This approximation is usually enough good approximation to make qualitative analysis and to obtain some quantitative results. All obtained results have been checked by comparison with the results of numerical simulations.

DISCUSSION

In this section, we analyzed the dynamics of redistributions of dopant and radiation defects during annealing and under influence of mismatch-induced stress and modification of porosity. Typical distributions of the concentrations of dopant in heterostructures are presented in Figures 2 and 3 for diffusion and ion types of doping, respectively. These distributions have been calculated for the case, when the value of dopant diffusion coefficient in doped area is larger than in nearest areas. The figures show that inhomogeneity of heterostructure gives us possibility to increase the compactness of concentrations of dopants and at the same time to increase homogeneity of dopant distribution in doped part of epitaxial layer. However, framework this approach of manufacturing of bipolar transistor, it is necessary

to optimize annealing of dopant and/or radiation defects. Reason of this optimization is following. If annealing time is small, the dopant did not achieve any interfaces between materials of heterostructure. In this situation, one cannot find any modifications of distribution of the concentration of dopant. If annealing time is large, distribution of the concentration of dopant is too homogenous. We optimize annealing time framework recently introduces approach.[12,29-36] Framework this criterion, we approximate real distribution of the concentration of dopant by step-wise function [Figures 4 and 5]. Farther, we determine the optimal values of annealing time by minimization of the following mean-squared error.

$$U = \frac{1}{L_x L_y L_z} \int_0^{L_x} \int_0^{L_y} \int_0^{L_z} \left[\begin{matrix} C(x,y,z,\Theta) \\ -\psi(x,y,z) \end{matrix} \right] d\,z\,d\,y\,d\,x\,, \quad (15)$$

Where, ψ (x,y,z) is the approximation function. Dependences of optimal values of annealing time on parameters are presented in Figures 6 and 7 for diffusion and ion types of doping, respectively.

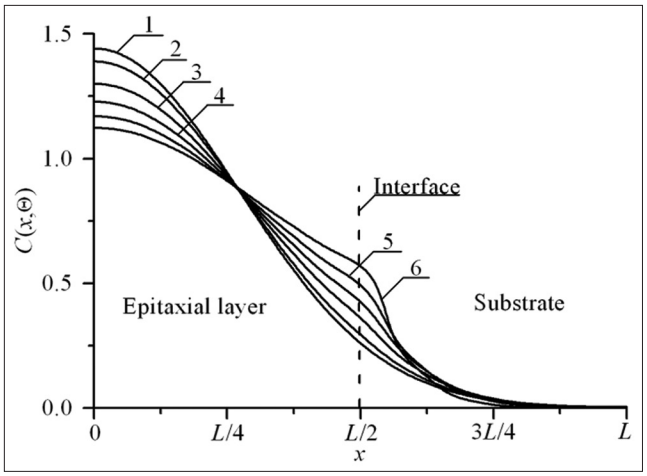

Figure 2: Distributions of the concentration of infused dopant in heterostructure from Figure 1 in direction, which is perpendicular to interface between epitaxial layer substrate. Increasing of the number of curve corresponds to increasing of difference between values of dopant diffusion coefficient in layers of heterostructure under condition, when the value of dopant diffusion coefficient in epitaxial layer is larger than the value of dopant diffusion coefficient in substrate

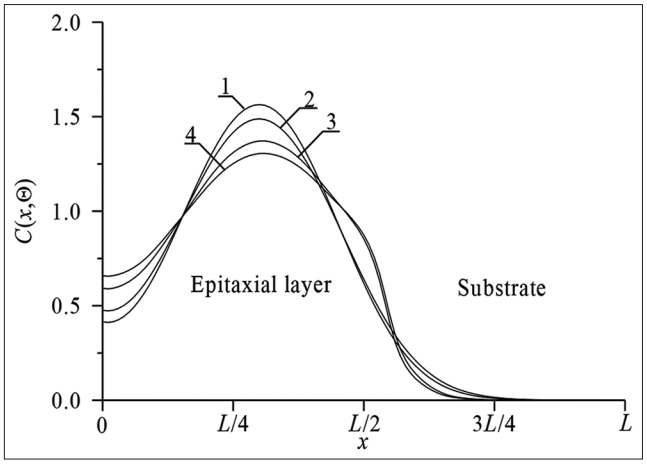

Figure 3: Distributions of the concentration of implanted dopant in heterostructure from Figure 1 in direction, which is perpendicular to interface between epitaxial layer substrate. Curves 1 and 3 correspond to annealing time $\Theta = 0.0048(L_x^2+L_y^2+L_z^2)/D_0$. Curves 2 and 4 correspond to annealing time $\Theta = 0.0057(L_x^2+L_y^2+L_z^2)/D_0$. Curves 1 and 2 correspond to homogenous sample. Curves 3 and 4 correspond to heterostructure under condition, when the value of dopant diffusion coefficient in epitaxial layer is larger than the value of dopant diffusion coefficient in substrate

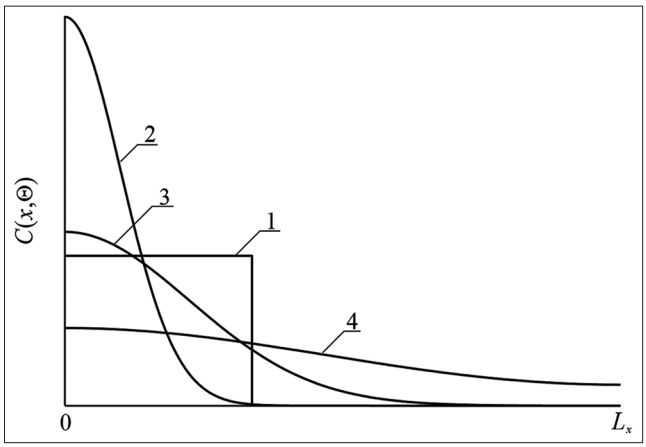

Figure 4: Spatial distributions of dopant in heterostructure after dopant infusion. Curve 1 is idealized distribution of dopant. Curves 2–4 are real distributions of dopant for different values of annealing time. Increasing of the number of curve corresponds to increasing of annealing time

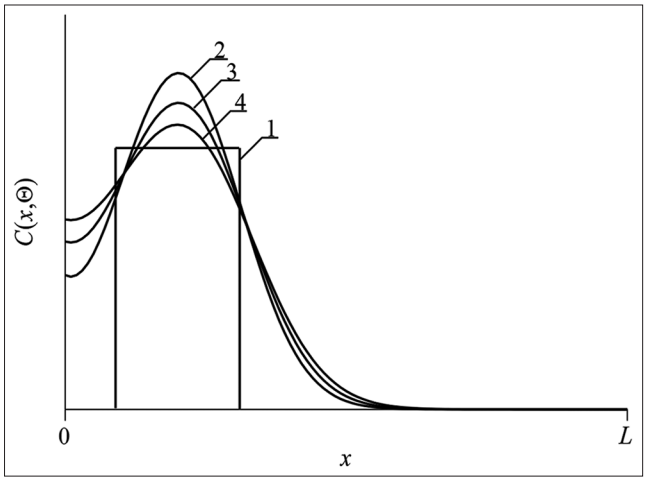

Figure 5: Spatial distributions of dopant in heterostructure after ion implantation. Curve 1 is idealized distribution of dopant. Curves 2–4 are real distributions of dopant for different values of annealing time. Increasing of number of curve corresponds to increasing of annealing time

It should be noted that it is necessary to anneal radiation defects after ion implantation. One could find spreading of the concentration of distribution of dopant during this annealing. In the ideal case, distribution of dopant achieves appropriate interfaces between materials of heterostructure during annealing of radiation defects. If dopant did not achieve any interfaces during annealing of radiation defects, it is practicably to additionally anneal the dopant. In this situation, optimal value of additional annealing time of implanted dopant is smaller than annealing time of infused dopant.

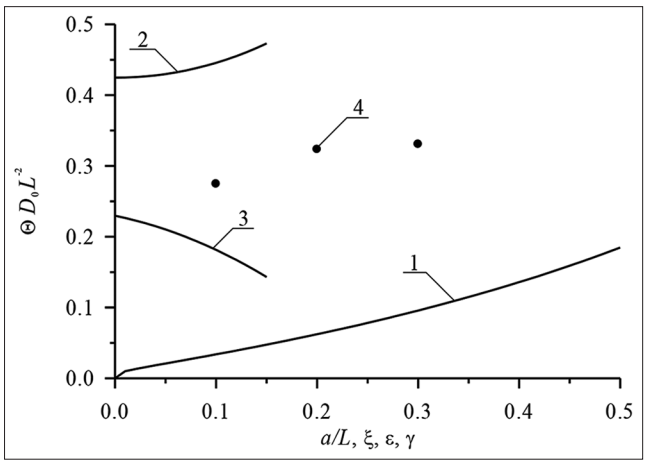

Figure 6: Dependences of dimensionless optimal annealing time for doping by diffusion, which have been obtained by minimization of mean-squared error, on several parameters. Curve 1 is the dependence of dimensionless optimal annealing time on the relation a/L and $\xi = \gamma = 0$ for equal to each other values of dopant diffusion coefficient in all parts of heterostructure. Curve 2 is the dependence of dimensionless optimal annealing time on value of parameter ε for a/L=1/2 and $\xi = \gamma = 0$. Curve 3 is the dependence of dimensionless optimal annealing time on value of parameter ξ for a/L=1/2 and $\varepsilon = \gamma = 0$. Curve 4 is the dependence of dimensionless optimal annealing time on value of parameter γ for a/L=1/2 and $\varepsilon = \xi = 0$

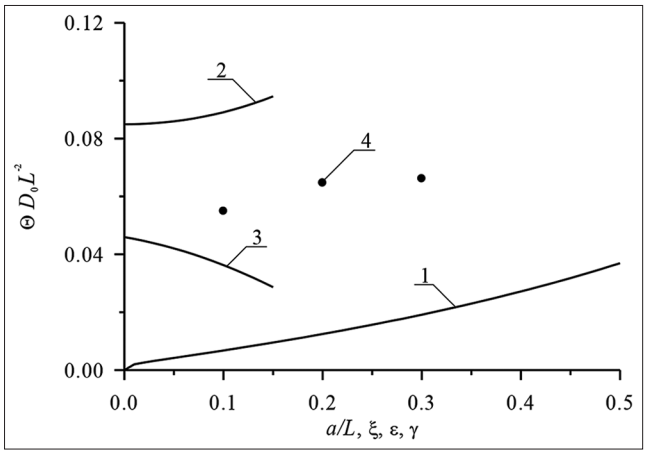

Figure 7: Dependences of dimensionless optimal annealing time for doping by ion implantation, which have been obtained by minimization of mean-squared error, on several parameters. Curve 1 is the dependence of dimensionless optimal annealing time on the relation a/L and $\xi = \gamma = 0$ for equal to each other values of dopant diffusion coefficient in all parts of heterostructure. Curve 2 is the dependence of dimensionless optimal annealing time on value of parameter ε for a/L=1/2 and $\xi = \gamma = 0$. Curve 3 is the dependence of dimensionless optimal annealing time on value of parameter ξ for a/L=1/2 and $\varepsilon = \gamma = 0$. Curve 4 is the dependence of dimensionless optimal annealing time on value of parameter γ for a/L=1/2 and $\varepsilon = \xi = 0$

Farther, we analyzed influence of relaxation of mechanical stress on distribution of dopant in doped areas of heterostructure. Under following condition, $\varepsilon_0 < 0$, one can find compression of distribution of concentration of dopant near interface between materials of heterostructure. Contrary (at $\varepsilon_0 > 0$), one can find spreading of distribution of concentration of dopant in this area. This changing of distribution of concentration of dopant could be at least partially compensated using laser annealing.[36] This type of annealing gives us possibility to accelerate diffusion of dopant and another processes in annealed area due to inhomogeneous distribution of temperature and Arrhenius law. Accounting relaxation of mismatch-induced stress in heterostructure could lead to changing of optimal values of annealing time. At the same time, modification of porosity gives us possibility to decrease value of mechanical stress. On the one hand, mismatch-induced stress could be used to increase density of the elements of integrated circuits and, on the other hand, could lead to generation dislocations of the discrepancy. Figures 8 and 9 show the distributions of concentration of vacancies in porous materials and component of displacement vector, which is perpendicular to interface between the layers of heterostructure.

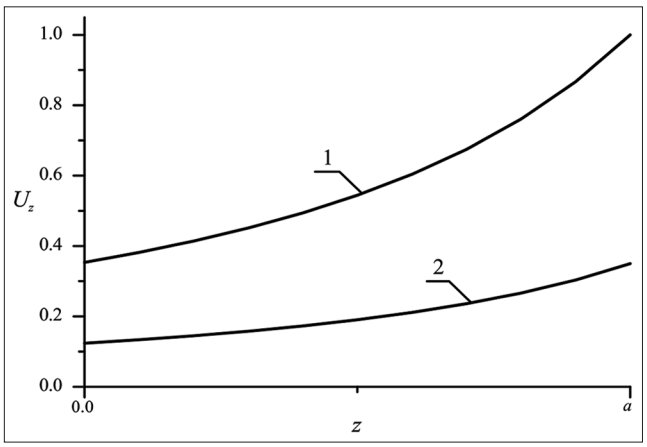

Figure 8: Normalized dependences of component u_z of displacement vector on coordinate z for non-porous (curve 1) and porous (curve 2) epitaxial layers

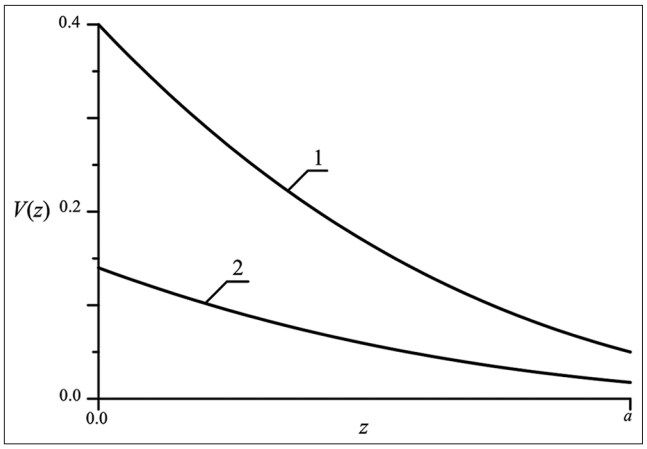

Figure 9: Normalized dependences of vacancy concentrations on coordinate *z* in unstressed (curve 1) and stressed (curve 2) epitaxial layers

CONCLUSION

In this paper, we model redistribution of infused and implanted dopants with account relaxation mismatch-induced stress during manufacturing field-effect heterotransistors framework a four-stage distributed amplifier. We formulate recommendations for optimization of annealing to decrease dimensions of transistors and to increase their density. We formulate recommendations to decrease mismatch-induced stress. Analytical approach to model diffusion and ion types of doping with account concurrent changing of parameters in space and time has been introduced. At the same time, the approach gives us possibility to take into account non-linearity of considered processes.

REFERENCES

1. Lachin VI, Savelov NS. Electronics. Rostov-On-Don: Phoenix; 2001.
2. Polishscuk A. Programmable analog IC anadigm: The whole range of analog electronics on a single chip. First meeting. Mod Electron 2004;12:8-11.
3. Volovich G. Modern models of integrated operational amplifiers. Mod Electron 2006;2:10-7.
4. Kerentsev A, Lanin V. Constructive and technological features of MOSFET-transistors. Power Electron 2008;1:34.
5. Ageev AO, Belyaev AE, Boltovets NS, Ivanov VN, Konakova RV, Kudrik YY, *et al*. Au-TiB x-n-6H-SiC Schottky barrier diodes: Specific features of charge transport in rectifying and nonrectifying contacts. Semiconductors 2009;43:897-903.
6. Tsai JH, Chiu SY, Lour WS, Guo DF. High-performance InGaP/GaAs pnp δ-doped heterojunction bipolar transistor. Semiconductors 2009;43:971-4.
7. Alexandrov OV, Zakhar'in AO, Sobolev NA, Shek EI, Makoviychuk MM, Parshin EO. Formation of donor centers upon annealing of dysprosium and holmium-implanted silicon. Semiconductors 1998;32:1029-32.
8. Ermolovich IB, Milenin VV, Red'ko RA, Red'ko SM. Features of recombination processes in CdTe films fabricated at different temperature conditions of growth and subsequent annealing. Semiconductors 2009;43:1016-20.
9. Sinsermsuksakul P, Hartman K, Kim SB, Heo J, Sun L, Park HH, *et al*. Enhancing the efficiency of SnS solar cells via band-offset engineering with a zinc oxysulfide buffer layer. Appl Phys Lett 2013;102:053901-5.
10. Reynolds JG, Reynolds CL, Mohanta A Jr., Muth JF, Rowe JE, Everitt HO, Aspnes DE. Shallow acceptor complexes in p-type ZnO. Appl Phys Lett 2013;102:152114-8.
11. Volokobinskaya NI, Komarov IN, Matyukhina TV, Reshetnikov VI, Rush AA, Falina IV, *et al*. A study of technological processes in the production of high-power high-voltage bipolartransistors incorporating an array of inclusions in the collector region. Semiconductors 2001;35:1013-7.
12. Pankratov EL, Bulaeva EA. Doping of materials during manufacture p-n-junctions and bipolar transistors. Analytical approaches to model technological approaches and ways of optimization of distributions of dopants. Rev Theor Sci 2013;1:58-82.
13. Kukushkin SA, Osipov AV, Romanychev AI. Epitaxial zinc oxide growth by molecular layering on SiC/Si substrates. Phys Solid State 2016;58:1448-52.
14. Trukhanov EM, Kolesnikov AV, Loshkarev ID. Long-range stresses generated by misfit dislocations in epitaxial films. Russ Microelectron 2015;44:552-8.
15. Pankratov EL, Bulaeva EA. About some ways to decrease quantity of defects in materials for solid state electronic devices and diagnostics of their realization. Rev Theor Sci 2015;3:365-98.
16. Ong KK, Pey KL, Lee PS, Wee AT, Wang XC, Chong YF. Dopant distribution in the recrystallization transient at the maximum melt depth induced by laser annealing. Appl Phys Lett 2006;89:172111-4.
17. Wang HT, Tan LS, Chor EF. Pulsed laser annealing of Be-implanted GaN J Appl Phys 2006;98:094901-5.
18. Bykov YV, Yeremeev AG, Zharova NA, Plotnikov IV, Rybakov KI, Drozdov MN, *et al*. Diffusion Processes in Semiconductor Structures During Microwave Annealing. Radiophys Quantum Electron 2003;43:836-43.
19. Piccinni G, Avitabile G, Talarico C, Coviello G. UWB distributed amplifier design using lookup tables and gm over ID methodology. Analog Integr Circ Sig Process 2017;90:615-24.
20. Zhang YW, Bower AF. Numerical simulations of island formation in a coherent strained epitaxial thin film system. J Mech Phys Solids 1999;47:2273-97.
21. Landau LD, Lefshits EM. Theoretical Physics, 7 (Theory of Elasticity). Moscow: Physmatlit; 2001.
22. Kitayama M, Narushima T, Carter WC, Cannon RM, Glaeser AM. The Wulff Shape of Alumina: I, Modeling the Kinetics of Morphological Evolution. J Am Ceram Soc 2000;83:2561-72.
23. Cheremskoy PG, Slesov VV, Betekhtin VI. Pore in

Solid Bodies. Moscow; Energoatomizdat; 1990.
24. Gotra ZY. Technology of Microelectronic Devices. Moscow: Radio and Communication; 1991.
25. Fahey PM, Griffin PB, Plummer JD. Point defects and dopant diffusion in silicon. Rev Mod Phys 1989;61:289-388.
26. Vinetskiy VL, Kholodar GA. Radiative Physics of Semiconductors. Kiev: Naukova Dumka; 1979.
27. Mynbaeva MG, Mokhov EN, Lavrent'ev AA, Mynbaev KD. High-temperature diffusion doping of porous silicon carbide. Tech Phys Lett 2008;34:13.
28. Sokolov YD. On the determination of dynamic forces in mine hoisting ropes. Appl Mech 1955;1:23-35.
29. Pankratov EL. Impurity dynamics in the formation of p-n-junctions in inhomogeneous structures. Optimization of annealing time. Russ Microelectron 2007;36:33-9.
30. Pankratov EL. Redistribution of dopant during annealing of radiative defects in a multilayer structure by laser scans for production an implanted-junction rectifiers. Int J Nanosci 2008;7:187-97.
31. Pankratov EL, Bulaeva EA. Decreasing of quantity of radiation defects in an implanted-junction rectifiers by using overlayers. Int J Micro-Nano Scale Transp 2012;3:119-30.
32. Pankratov EL, Bulaeva EA. Optimization of manufacturing of emitter-coupled logic to decrease surface of chip. Int J Mod Phys B 2015;29:1-12.
33. Pankratov EL. On approach to optimize manufacturing of bipolar heterotransistors framework circuit of an operational amplifier to increase their integration rate. Influence mismatch-induced Stress. J Comp Theor Nanosci 2017;14:4885-99.
34. Pankratov EL, Bulaeva EA. An approach to increase the integration rate of planar drift heterobipolar transistors. Mater Sci Semicond Process 2015;34:260-8.
35. Pankratov EL, Bulaeva EA. An approach to manufacture of bipolar transistors in thin film structures. On the method of optimization. Int J Micro-Nano Scale Transp 2014;4:17-31.
36. Pankratov EL. Synchronization of impurities infusion for production of a sequence of diffused-junction rectifiers. Nano 2011;6:31-40.